www.coinweb.no

SINTEF Building and Infrastructure Jan Arve Øverli (NTNU) og Tore Myrland Jensen

Confinement effect of fibres on the behaviour of lightweight aggregate concrete beams

COIN Project report 67 – 2015

SINTEF

SINTEF Building and Infrastructure

Jan Arve Øverli (NTNU) og Tore Myrland Jensen

Confinement effect of fibres on the behaviour of lightweight aggregate concrete beams

FA 3 Technical performance

SP 3.3 Structural performance

COIN Project report 67 – 2015

COIN Project report no 67
Jan Arve Øverli (NTNU) og Tore Myrland Jensen
Confinement effect of fibres on the behaviour of lightweight aggregate concrete beams
FA 3 Technical performance
SP 3.3 Structural performance

Keywords:
LWAC, Bending tests, Confinement, Ductility, Lightweight concrete, Fibre

Project no.: 102000442-8

Photo, cover: «Gallery», iStock

ISSN 1891–1978 (online)
ISBN 978-82-536-1467-0 (pdf)

Address: Forskningsveien 3 B
POBox 124 Blindern
N-0314 OSLO
Tel: +47 22 96 55 55
Fax: +47 22 69 94 38 and 22 96 55 08

www.sintef.no/byggforsk
www.coinweb.no

Cooperation partners / Consortium Concrete Innovation Centre (COIN)

Kværner Engineering
Contact: Jan-Diederik Advocaat
Email: Jan-Diederik.Advocaat@kvaerner.com
Tel: +47 67595050

Saint Gobain Weber
Contact: Geir Norden
Email: geir.norden@saint-gobain.com
Tel: +47 22887700

Norcem AS
Contact: Terje Rønning
Email: terje.ronning@norcem.no
Tel: +47 35572000

NTNU
Contact: Terje Kanstad
Email: terje.kanstad@ntnu.no
Tel: +47 73594700

Mapei AS
Contact: Trond Hagerud
Email: trond.hagerud@mapei.no
Tel: +47 69972000

SINTEF Building and Infrastructure
Contact: Tor Arne Hammer
Email: tor.hammer@sintef.no
Tel: +47 73596856

Skanska Norge AS
Contact: Sverre Smeplass
Email: sverre.smeplass@skanska.no
Tel: +47 40013660

Norwegian Public Roads Administration
Contact: Kjersti K. Dunham
Email: kjersti.kvalheim.dunham@vegvesen.no
Tel: +47 22073940

Unicon AS
Contact: Stein Tosterud
Email: stto@unicon.no
Tel: +47 22309035

Veidekke Entreprenør ASA
Contact: Christine Hauck
Email: christine.hauck@veidekke.no
Tel: +47 21055000

Preface

This study has been carried out within COIN - Concrete Innovation Centre - one of presently 14 Centres for Research based Innovation (CRI), which is an initiative by the Research Council of Norway. The main objective for the CRIs is to enhance the capability of the business sector to innovate by focusing on long-term research based on forging close alliances between research-intensive enterprises and prominent research groups.

The vision of COIN is creation of more attractive concrete buildings and constructions. Attractiveness implies aesthetics, functionality, sustainability, energy efficiency, indoor climate, industrialized construction, improved work environment, and cost efficiency during the whole service life. The primary goal is to fulfil this vision by bringing the development a major leap forward by more fundamental understanding of the mechanisms in order to develop advanced materials, efficient construction techniques and new design concepts combined with more environmentally friendly material production.

The corporate partners are leading multinational companies in the cement and building industry and the aim of COIN is to increase their value creation and strengthen their research activities in Norway. Our over-all ambition is to establish COIN as the display window for concrete innovation in Europe.

About 25 researchers from SINTEF (host), the Norwegian University of Science and Technology - NTNU (research partner) and industry partners, 15 - 20 PhD-students, 5 - 10 MSc-students every year and a number of international guest researchers, work on presently eight projects in three focus areas:

- Environmentally friendly concrete
- Economically competitive construction
- Aesthetic and technical performance

COIN has presently a budget of NOK 200 mill over 8 years (from 2007), and is financed by the Research Council of Norway (approx. 40 %), industrial partners (approx 45 %) and by SINTEF Building and Infrastructure and NTNU (in all approx 15 %).

For more information, see www.coinweb.no

Tor Arne Martius-Hammer
Centre Manager

Summary

This study focuses on ductility of lightweight aggregate concrete (LWAC) in compression. The major disadvantage of LWAC is the brittleness in compression at the material level compared to normal density concrete. Requirements for energy absorption and/or a controlled behaviour after peak load may exclude LWAC as the preferred material. In overload situations adequate ductility is essential to ensure safety. Floating offshore structures and LNG-terminals are often post-tensioned, e.g. to avoid leakage cracks in service. Thus the compressive ductility is of great importance. The influence of the stress-strain characteristics in compression is also more pronounced in structures subjected to combined bending moment and axial forces. Ductility of LWAC in compression plays an important part in improving the structural ductility in heavily reinforced and post-tensioned structures. Increase of the ductility in the compression zone in bending is possible by employing stirrups and/or fibre reinforcement to achieve passive confinement.

To study the ductility an experimental program was set up consisting of eight over-reinforced light-weight concrete beams with length 4200 mm and cross-section 300×200 mm, which were subjected to four-point bending. The beams were heavily over-reinforced to ensure spalling in the compression zone of the cross section before yielding of the tensile reinforcement. The LWAC had a mass density about 1800 kg/m^3, with a compressive strength about 40 MPa. Four different confinement configurations of the compression zone of the beams were investigated - only LWAC and three different types of fibre, 60 and 35 mm long steel fibres and basaltic fibres, all with 1% of fibre. This report presents mainly the results from the experimental investigation of the beams, with focus on the flexural response. The effect of the different confinement configurations is analysed in detail in the plastic hinge region.

The pre-peak response before initiation of spalling was approximately the same for all configurations. The spalling load was identified as the load where horizontal cracking in the compressive zone occurred. This load level was the same as the peak load for the response. An approximately 10% increase in load capacity was observed for the beams with fibre which is due to the confinement effect.

As expected, the reference beams with only LWAC in the compression zone, had a brittle post-peak response, i.e. no post-peak deformability and a very steep descending branch immediately after initiation of spalling of the concrete cover. Also the beams with different type of fibre experienced a decreased capacity after the peak load. However, some ductility was achieved, especially for the beams with steel fibres. The beams with basaltic fibres responded with a drop in capacity after peak load before gaining some deformation capacity.

The results from this investigation show that fibres do contribute to the confinement in the compressive zone. However, an acceptable ductility to be used in structural design was not achieved for the beams in this project. The ductility is influenced by many factors such as size of cross-section, curvature and amount of fibre. More research is required before conclusions can be made that LWAC have potential to be consistent with the performance requirements for structural materials with respect to ductility.

Keywords: Bending tests, Confinement, Ductility, Lightweight concrete, Fibre

Table of contents

1 Introduction

Lightweight aggregate concrete (LWAC) has been used as a construction material for many decades. The main objective for using LWAC is normally to reduce cost by reducing the dead load of structures. E.g. with low weight the dimensions of the foundations in buildings can be reduced in areas with low bearing capacities, the inertia actions are reduced in seismic regions and it enables easier handling and transportation of precast elements. Even with the major advantage of reduced weight and the high strength-to-weight ratio of the material compared to conventional concrete, the use of LWAC is still limited as a mainstream construction material in the building industry. However, for large and advanced structures like high rise buildings, bridges and offshore structures it has been applied with great success [1]. Other advantages of LWAC compared to normal weight concrete are the improved durability properties, fire resistance and the low thermal conductivity.

The major disadvantage of LWAC is the brittleness in compression at the material level compared to normal density concrete. Adequate strength, which easily can be fulfilled with lightweight concrete, is not the only required design criteria. In overload situations adequate ductility is essential to ensure safety. Ductility is defined as individual structural members or entire structures ability to sustain significant inelastic deformations after peak load without a significant loss in the capacity prior to failure. This is of great importance in redistribution of forces and a major consideration in design of structures in seismic areas. The limited post peak behaviour of LWAC can explain the limited use of the material for practical purposes. Requests for energy dissipation and/or a controlled behaviour after peak load can therefore exclude LWAC as the preferred material.

It is well known that confinement increases the ductility of concrete in addition to enhancing the concrete strength. Active confinement from external stresses is more effective than passive confinement which is mobilised by opposing transverse deformation from the Poisson effect. In reinforced concrete the passive confinement from transverse reinforcement is the most common. Numerous researchers have investigated both experimental and theoretical, the effect of ordinary transverse steel reinforcement and the effect of adding fibres on the confinement in normal density concrete [2-7]. For lightweight aggregate concrete similar effects is reported [8-10]. The effect of confinement is also taken into account in design codes for concrete structures [11]. However, most studies on confinement focus on columns and cylinders subjected only to uniaxial loading [12-14]. Flexural behaviour of LWAC beams with focus on ductility has been reported, but only on under-reinforced beams [15-19].

The main objective in this study is to investigate the passive confinement effect of different types of fibres on the ductility in LWAC structures. In another COIN project the effect of fibres and/or closed links on the flexural ductility in LWAC beams is already documented, concluding that fibres have a significant effect on the ductility [20]. However, only one type of fibre, steel fibres with length 60mm was investigated. As an extension the focus now is on the effect of different fibre types on the compressive ductility. An experimental program was set up consisting of eight over-reinforced concrete beams, which were subjected to four-point bending. Four different configurations of the beams were investigated to study the response. Two beams have only LWAC and considered reference beams, two beams each with 60mm and 35mm long steel fibres respectively, and two beams with basaltic fibres with length 45mm.

This experimental program is considered a first step on investigating the ductility of LWAC structures. Only static loading is considered, even if repeated loading is very important to assess structural integrity in seismic areas. Confinement and ductility of LWAC in general is

well documented in the literature. However, information dealing with ductility of over-reinforced LWAC structures in bending or structures subjected to combined bending and membrane action is limited. The experimental work has been carried out as part of two Master theses at the Department of Structural Engineering at the Norwegian University of Science and Technology [21-23].

2 Experimental program

2.1 Overview – beam design

The test programme was designed to study the confinement effect of different types of fibres on the ductility in heavily reinforced lightweight aggregate concrete beams. The main focus was on the ductility in the compression zone; thus, the beams were heavily reinforced to ensure a bending failure in the compression zone of the cross section before the tensile reinforcement yielded.

The experimental programme consisted of eight simply supported concrete beams, which were tested in flexure under a four-point loading system, see Fig. 1. Hence, the central part of the beam was in pure bending mode, which was the main focus of this work. The free span between the supports was 3.6 m, and two concentrated loads were symmetrically applied at a distance of 0.8 m. Four different configurations of the LWAC beams were investigated to study the response. Two beams with only LWAC were considered as the reference beams (Beam 1), two beams had 65 mm long steel fibres (Beam 2), and two had 35 mm long steel fibres (Beam 3), whereas the final two beams had basaltic fibres (Beam 4). The two beams in each configuration were identical.

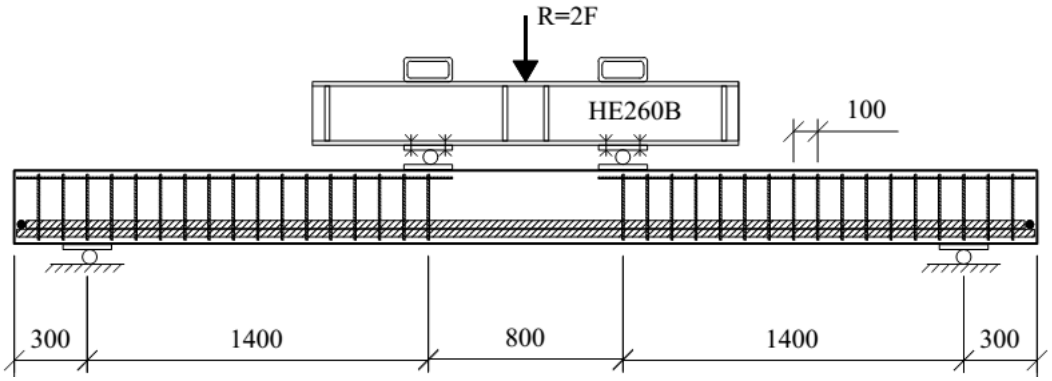

***Figure 2.1**: Loading arrangement, reinforcement layout and dimensions (in mm)*

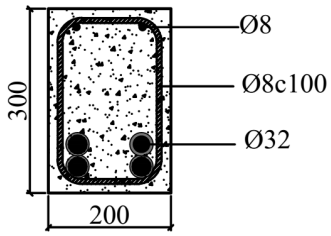

***Figure 2.2**: Reinforcement layout and dimensions (in mm)*

The cross sections in the beams were rectangular, 200 mm wide and 300 mm deep. The total length of the beams was 4.2 m and they were simply supported over a span of 3.6 m. The beams were designed to be over-reinforced, hence, the longitudinal tensile reinforcement should not yield at failure. To achieve this, four deformed bars with diameter 32 mm was required. As seen in Figure 2.2 they were arranged as bundles of two bars at each side. In the compression zone 2 bars with diameter 12 mm was placed in one layer in the shear span. To ensure enough anchoring capacity a transverse horizontal bar with diameter 32 mm was welded on the bottom layer of the tensile reinforcement at the ends of the beams.

The aim of this work is to study the ductility in compression. Thus, in the shear spans between the load point and the support all beams were provided stirrups with spacing 100mm to ensure flexural failure. Transverse reinforcement consisted of 10 mm diameter deformed bars bent into closed stirrups. The concrete cover to the stirrups was 15mm.

2.2 Materials and mix proportions

The LWAC in the project were designed and prepared in-house. The two beams in each beam configuration were produced from the same batch. To produce the concrete, lightweight expanded clay aggregate, commercially known as LECA, was used to achieve the desired density of the LWAC. The project aimed for a mean compressive strength of ~ 40 MPa and a density of the LWAC of ~1800 kg/m^3.

The concrete mix is given in Table 2.1. The mix was the same for all beams. The LECA 2-4 and 4-8mm have bulk densities of 380 kg/m^3 and 800 kg/m^3 respectively. To improve paste/cement and fibre/concrete bonds the mix contained silica fume of 10 % by weight of the cement. In addition limestone powder was added to avoid segregation. The sand had a high content of fines to increase the workability and to stabilise the concrete.

Three types of fibre where used for the different beam types, Dramix 65/60 (D-65) and KrampeHarex 35/0.6 55H (K-35) steel fibre, and basaltic fibre. Both types of steel fibres were cold drawn wire fibre of bright steel with hooked ends. The fibre content was 78 kg/m^3 and 19 kg/m^3 for the steel and basaltic fibre respectively, which corresponds to an amount of fibres of 1 % by volume of concrete. The mechanical properties for the fibres are given in Table 2.3.

The moisture content and the absorbed water in the LECA were measured, and are necessary input when designing the concrete mix. The two fractions of LECA were homogenised separately in a drum and sealed in plastic bags. Thus, the LECA in each concrete batch had almost the same moisture content.

***Table 2.1**: Concrete mix proportions for LWAC*

Constituent	Weight [kg/m^3]
Cement (CEM I)	434.9
Silica fume	43.5
Limestone powder	4.3
Water (free)	198.3
Absorbed water	10.7
LECA 2-4mm	133.5
LECA 4-8mm	237.8
Sand 0-8mm	432.8
Filler sand	270.5
Superplasticiser	7.8
Fibre steel/basalt	78/19

The mixing was done using a 0.8 m^3 laboratory mixer. First cement, silica fume, LECA and sand were mixed for approximately 2 min. Water was added and the superplasticiser was continuously added and adjusted during mixing, until the desired workability of the concrete was achieved. Finally, fibres were carefully spread in the mixer to achieve a uniform distribution of the fibres in the concrete.

2.3 Mechanical properties

Mechanical properties were obtained for the LWAC for the different batches. For each beam six cylinders with diameter 100 mm and height 200 mm were casted to find the compressive strength and density of LWAC at the day of testing (cylinders stored together with the beams). The strength and the density were found according to the standards in [24] and [25] respectively. Table 2.2 presents the obtained mean mechanical properties from tests at the same day as testing of the beams.

***Table 2.2**: Mechanical properties for different mixes*

Beam no. and configuration	f_{lcm} (MPa)	Density, ρ_l (kg/m^3)	Oven-dry density, ρ (kg/m^3)
1: Only LWAC	41.0	-	-
2: D-65	39.1	1781	1659
3: K-35	40.0	1828	1686
4: B-45	40.5	1785	1634

***Table 2.3**: Mechanical properties for fibres*

Fibre type	f_y (MPa)	E (GPa)	Density (kg/m^3)	Length (mm)	Diameter (mm)
Dramix 65/60	1160	210	7800	60	0.90
KrampeHarex 35/0.6 55H	2400	210	7800	35	0.60
Basalt Minibars gen3	1100	60	1900	45	1.02

The beams in this project are over-reinforced. Hence, the yield strain and Young's modulus of elasticity of the longitudinal reinforcement are important parameters. To be able to evaluate the results and to compare the strains from the experiments with calculations, deformed bar with diameter 32 mm was tested according to [26] in an earlier project [20] to characterize the properties. Figure 2.3 shows the stress-strain relationships from the tests as mean values for three tests. The bar with diameter 10mm has an almost perfect linear-ideal plastic behaviour. As expected the bars with diameter 32mm shows a more non-linear behaviour before reaching the yield stress of 565 MPa at a strain of 3.75‰. Young's modulus is approximately 188 GPa, calculated from the linear part of the stress-strain diagram.

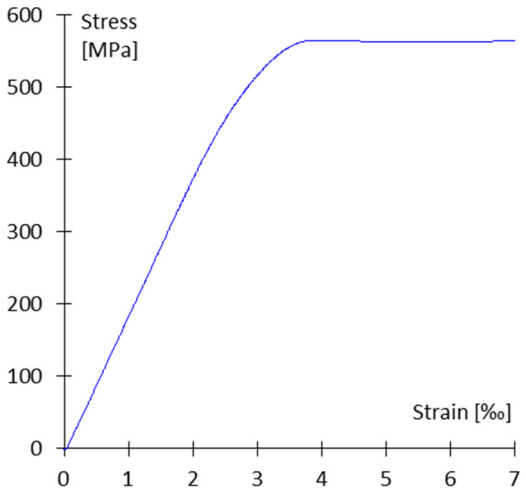

***Figure 2.3**: Stress-strain relationships for reinforcement Ø32*

2.4 Residual flexural tensile strength, FRLWAC

For the beams with steel fibre, six small scale beams were casted from the same concrete batch as the large beams, to investigate the residual flexural tensile strength in accordance with [27]. The tests are based on simply supported beams with a free span of 0.5 m and a square cross section of 0.15 m, subjected to three point bending. The beams have a 25 mm deep notch at the middle point to initiate cracking. The results are presented in Figure 2.5 by using the crack mouth opening displacement (CMOD). In bending design of steel fibre reinforced concrete structures the residual flexural strength at a $CMOD_1$ of 2.5 mm, f_{R3}, is often used [28, 29]. The mean values of f_{R3} were 6.5, 6.5 and 2.1 MPa , with a relative standard deviation of 14%, 16% and 19 % for the three series respectively, see Table 2.4.

***Table 2.4**: Flexural strength and residual flexural strength at testing (MPa)*

	Small scale beam no.	X1	X2	X3	X4	X5	X6	Mean value	Std. (%)
Beam 2	Max flex. str. $f_{R,max}$	6.0	8.0	7.1	6.1	7.9	7.8	7.1	11.6
	$CMOD_1$: Res. flex. str. f_{R1}	5.8	7.5	6.3	6.0	7.5	7.3	6.8	10.6
	$CMOD_2$: Res. flex. str. f_{R2}	5.8	7.3	7.0	5.9	7.8	6.8	6.7	11.6
	$CMOD_3$: Res. flex. str. f_{R3}	5.3	7.0	7.0	5.8	7.7	6.4	6.5	14.1
	$CMOD_4$: Res. flex. str. f_{R4}	4.8	6.7	6.8	5.5	7.7	5.9	6.2	17.3
Beam 3	Max flex. str. $f_{R,max}$	7.5	7.5	7.1	7.7	6.6	10.4	7.8	12.7
	$CMOD_1$: Res. flex. str. f_{R1}	7.4	7.4	6.9	7.6	6.6	9.9	7.7	11.8
	$CMOD_2$: Res. flex. str. f_{R2}	7.0	6.8	6.3	7.0	5.8	10.2	7.2	15.2
	$CMOD_3$: Res. flex. str. f_{R3}	5.9	6.1	5.9	6.3	4.9	9.7	6.5	16.9
	$CMOD_4$: Res. flex. str. f_{R4}	5.2	5.6	5.2	5.4	4.2	9.0	5.8	18.2
Beam 4	Max flex. str. $f_{R,max}$	5.6	6.3	6.2	5.7	5.8	6.9	6.1	7.1
	$CMOD_1$: Res. flex. str. f_{R1}	5.5	6.2	6.1	5.6	5.7	6.7	6.0	6.9
	$CMOD_2$: Res. flex. str. f_{R2}	2.5	3.6	3.5	2.7	3.3	4.0	3.3	14.3
	$CMOD_3$: Res. flex. str. f_{R3}	1.6	2.2	2.1	1.7	1.7	3.2	2.1	18.8
	$CMOD_4$: Res. flex. str. f_{R4}	1.0	1.5	1.7	1.3	1.1	2.3	1.5	20.4

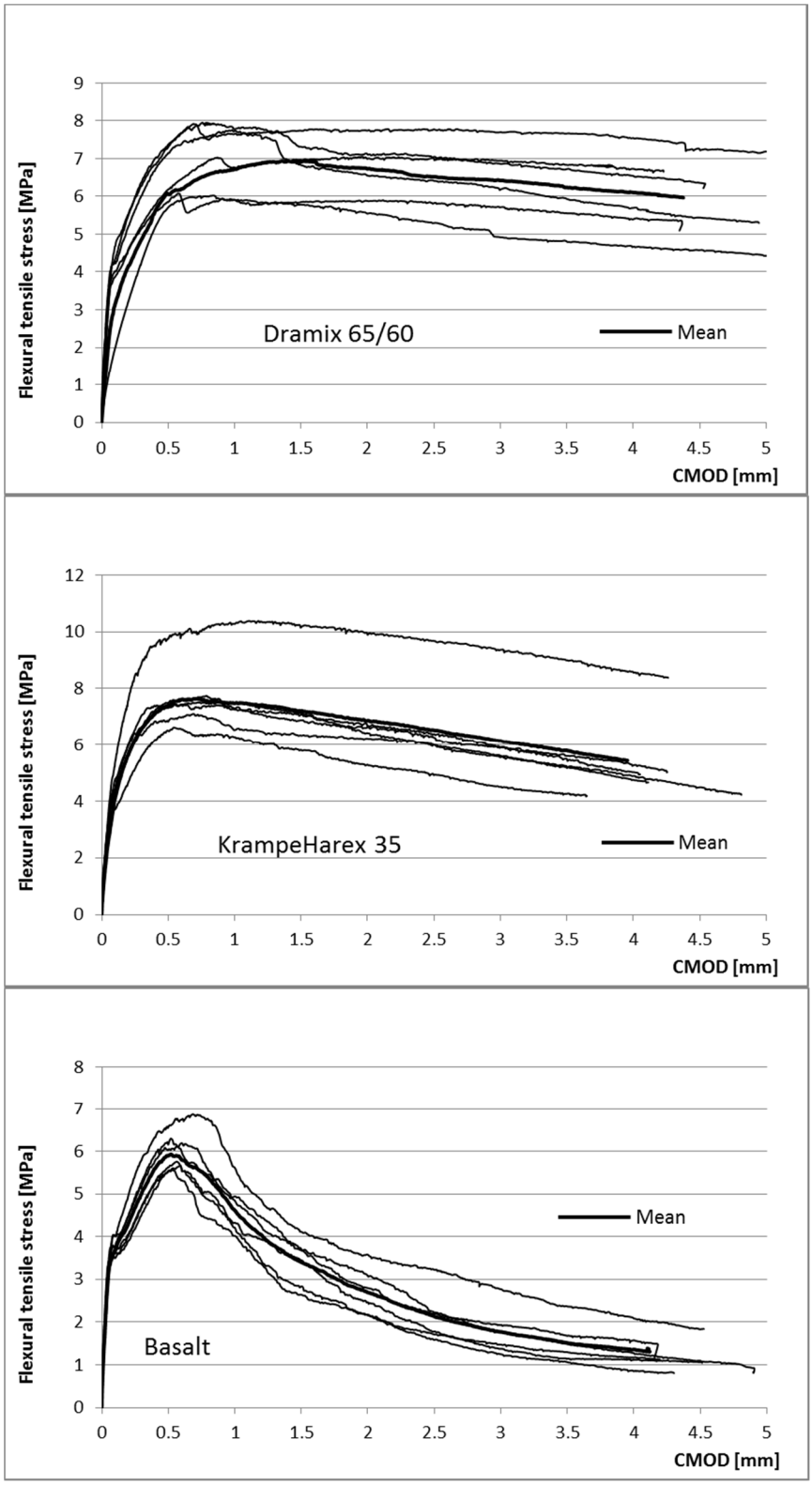

***Figure 2.4**: Flexural tensile strength - CMOD diagrams*

The relatively large scatter of results in Figure 2.4 is an indication on poor dispersion of the fibres in the beams. The fibre distribution in the cross-section was found by counting the number of fibres in a 25 mm top layer, a 100 mm middle layer and a 25 mm bottom layer of

the cross-section, see Appendix A3. The mean values for the number of fibres were 1.03 pr cm^2 for Dramix 65/60, 2.21 pr cm^2 for KrampeHarex 35, and 0.78 pr cm^2 for Basalt. However, only the numbers of fibres were registered. No attempt was made to find a fibre orientation factor.

2.5 Instrumentation and test procedure

The beams were suitably instrumented to measure displacements and strains, see Fig. 4. Deflections of the beams were measured at the mid span and at the load transfer points by three vertical linear variable differential transformers (LVDT), IS5-IS7. To help capture the concrete strains, four LVDTs were placed horizontally at the top and bottom levels on both sides of the cross section, IS1-IS4. They measured the longitudinal displacements over a distance of 0.5 m.

The load was applied by a 1000kN servo-controlled hydraulic actuator, and distributed to the LWAC beam by a steel beam (equalizer beam) with two rolled supports, see Fig. 1. At an initial stage, the beams were preloaded with a very small load to remove any slack in the system. The load was then released, all instruments were zeroed and the beams were loaded at a rate of 1.0 mm/min. Up to a load level of 75 kN, the loading was applied in intervals of 25 kN, whereas above 75 kN, the beams were continuously loaded until failure. All displacement, strain and load readings were automatically logged with a rate of 1.0 Hz

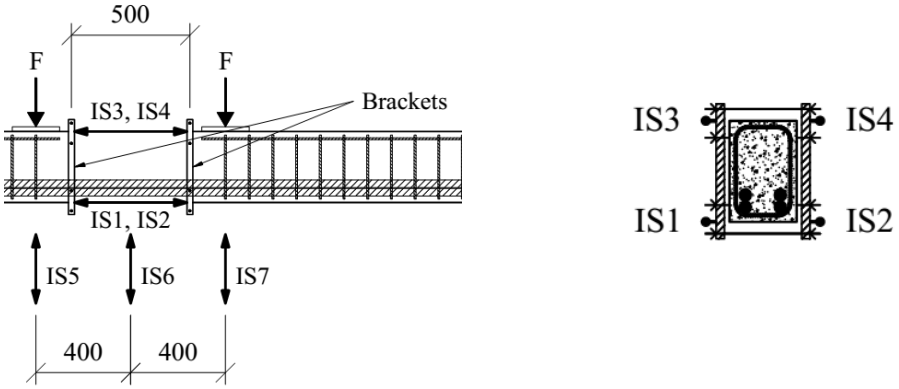

Fig. 2.5: Instrumentation of beams with LVDTs (IS1 to IS7) (dimensions in mm)

3 Test results and discussion

3.1 Main results

Table 3.1 summaries the main experimental results and calculations of the full scale tests regarding load capacity and displacement at mid span.

***Table 3.1**: Main experimental results and calculations*

Configuration and beam no:		Material LWAC [1]		Experimental results, capacity [2]			Experimental results, displacements at mid span [2]				Calculations, load capacity [3]		
		ρ [kg/m³]	f_{lcm} [MPa]	P_{spall} [kN]	M_{spall} [kNm]	$\varepsilon_{lc,spall}$ [‰]	Δ_{spall} [mm]	$\Delta_{0,85spall}$ [mm]	$\Delta_{0,6spall}$ [mm]	$\Delta_{0,85spall}/\Delta_{spall}$	$\Delta_{0,6spall}/\Delta_{spall}$	$P_{spall,calc}$ [kN]	$P_{spall}/P_{spall,calc}$	ε_{lcu3} [‰]
Only LWAC	Beam 1A	1610	41,0	99,1	141,3	2,90	22,0	[4]	[4]	[4]	[4]	104	0,950	2,94
	Beam 1B	1610	41,0	94,5	134,8	2,80	20,9	[4]	[4]	[4]	[4]	104	0,906	2,94
Dramix 65/60	Beam 2A	1610	39,1	111,8	159,0	3,13	25,1	30,0	43,0	1,195	1,714	100	1,116	2,94
	Beam 2B	1610	39,1	103,0	146,7	3,04	23,3	27,7	44,2	1,192	1,898	100	1,028	2,94
KrampeHarex 35	Beam 3A	1670	40,0	106,3	151,3	3,05	22,5	23,6	29,4	1,050	1,306	102	1,038	2,99
	Beam 3B	1670	40,0	106,9	152,1	3,07	23,4	27,7	39,9	1,186	1,709	102	1,043	2,99
Basaltic fibre	Beam 4A	1630	40,5	108,9	155,1	3,25	24,3	26,3	29,1	1,080	1,194	103	1,054	2,96
	Beam 4B	1630	40,5	107,9	153,7	3,13	23,8	35,7	30,0	1,078	1,260	103	1,045	2,96

1) Mean values from Chapter 2.3.1 (used in calculations)
2) Load-displacement relationship, see figures in Chapter 3.2 and Appendix A1
3) Calculation according to Eurocode 2 [30]. The fibre contribution to the ultimate compressive strain is not taken into account
4) Not relevant due to brittle behaviour at spalling and drop in load capacity (no real post-peak capacity achieved)

3.2 Load-displacement relationships

To investigate and describe the response of the tested beams, references will be made to the principal bending response of the over-reinforced concrete beams. The response can be characterized by five stages:

1. Before concrete cracks
2. Linear response for a cracked cross-section-B
3. Non-linear response before reaching the compressive capacity (strain limit) of the beam which initiate the spalling in the compressive zone, P_{spall}
4. A very brittle behaviour for beams with only LWAC, with confinement a more ductile post–peak behaviour

For an over-reinforced beam of LWAC, stage three is almost linear due to the more linear behaviour in compression of LWAC. The load-displacement curves for the centre point are given in Figure 3.1 for all eight beams. As expected beams with only LWAC, beam 1A and 1B, have a very brittle response after reaching maximum capacity (load at spalling). The spalling is identified when horizontal cracks develops in the compressive zone. The two beams (A and B) with the same type of fibre show in the post-peak behaviour. Especially Beam 3 with the 35 mm long steel fibres have a large difference. This is most likely due to the bad compaction during casting and fibre distribution and orientation. In casting of the beams there were differences in workability of the concrete which influence fibre distribution and orientation. However, even if registration of distribution and fibres were not performed this is an indication of the importance of fibre content on the compressive ductility.

From the normalized result in Figure 3.1b) there is clearly a difference between the basaltic fibres and the steel fibres. The different lengths of the steel fibre do not influence the result. The basaltic fibre has a more brittle post-peak response. The passive confinement effect from the fibres is influenced by the stiffness of the fibres. Since the basaltic fibre has a much lower elastic modulus, they need a larger transversal deformation to achieve the same confinement effect as steel fibres. This can be seen in the Figure 3.1, where after a drop in the capacity the beams with basaltic fibres are able to gain some ductility.

The responses for the beams demonstrate the influence of the different fibre types on the behaviour after spalling. Before spalling there is no significant influence of the fibre types. The beams with fibres have an approximately 10% increase in the capacity compared to the beams without fibre. This is in accordance with an earlier study [20]. Thus, the fibres have confinement effects which increase the compressive strength of the concrete.

Load-displacement curves and load-time curves, as illustrated in Figure 3.1 and 3.2 respectively, are shown separate for each beam in Appendix A1.

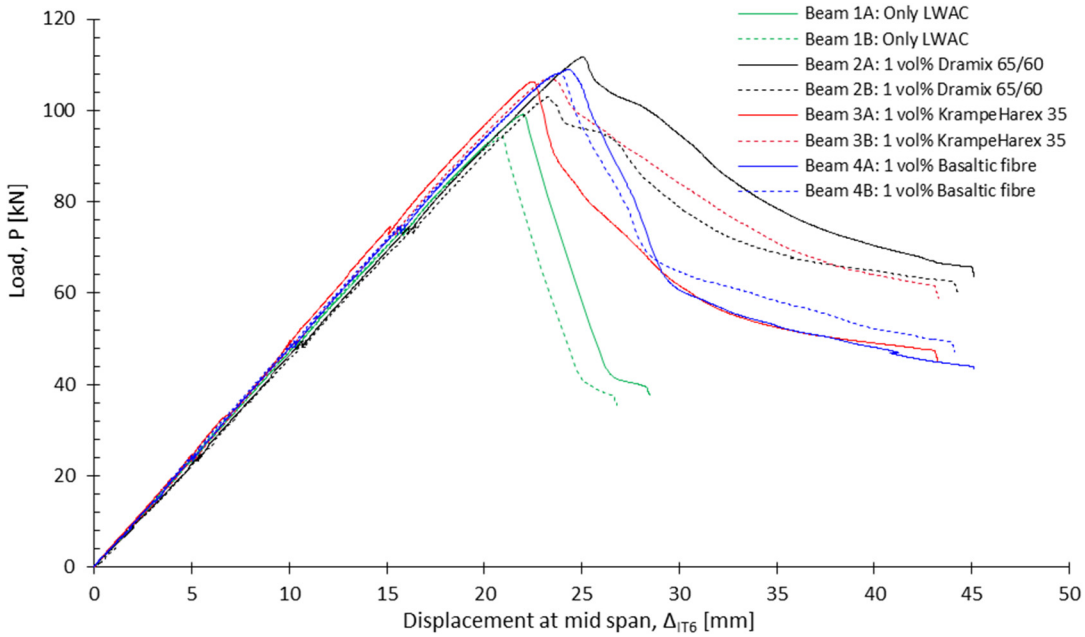

a) *Load-displacement curves*

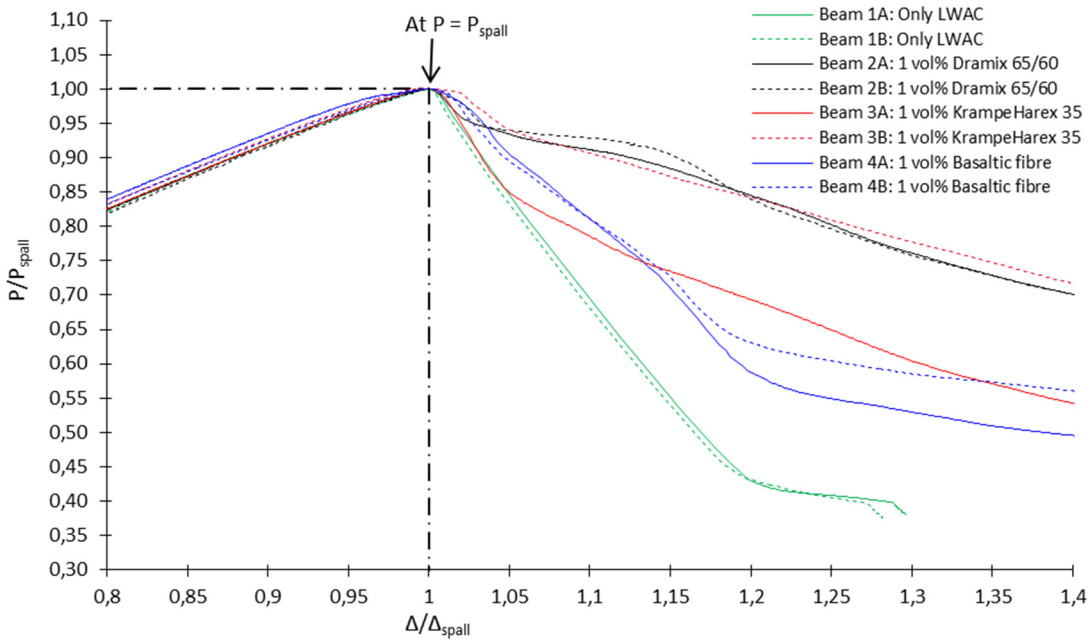

b) *Section of the normalized load-displacement curves around* P_{spall}

Figure 3.1*: Load-displacement curves for all beams at mid span*

As previously described the tests are performed with deformation controlled loading in load steps up towards spalling, and with continuous loading at- and after spalling. This loading procedure can clearly be seen in the load-time curves in Figure 3.3. The difference in load response between the beams at and after spalling, P_{spall}, are even clearer in the load-time curves than in the load-displacement curves. The beam without any fibre is completely brittle.

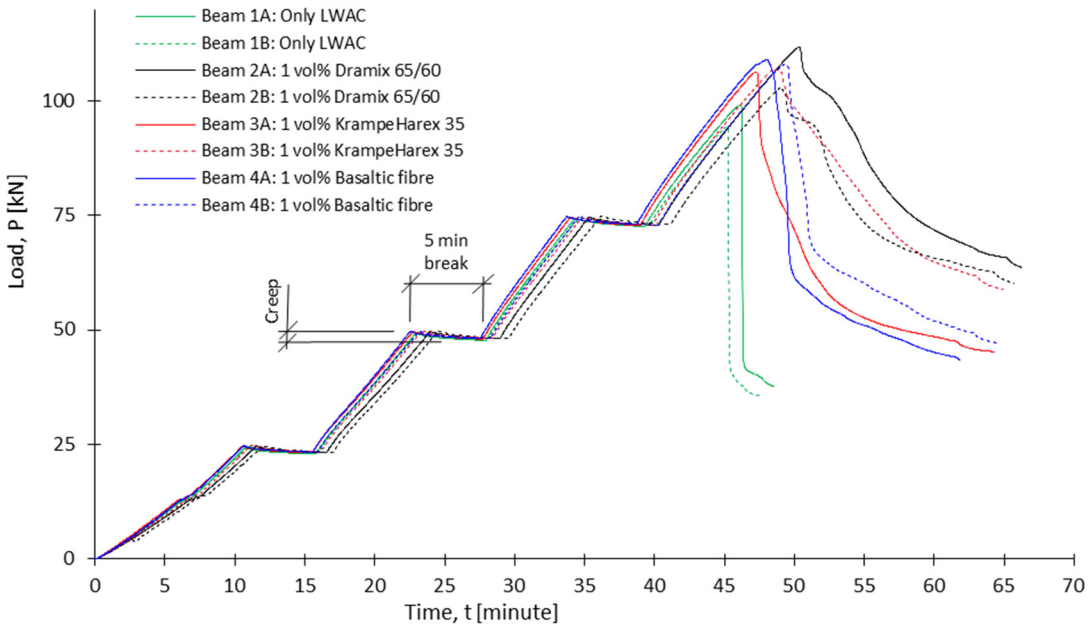

a) *Load-time curves*

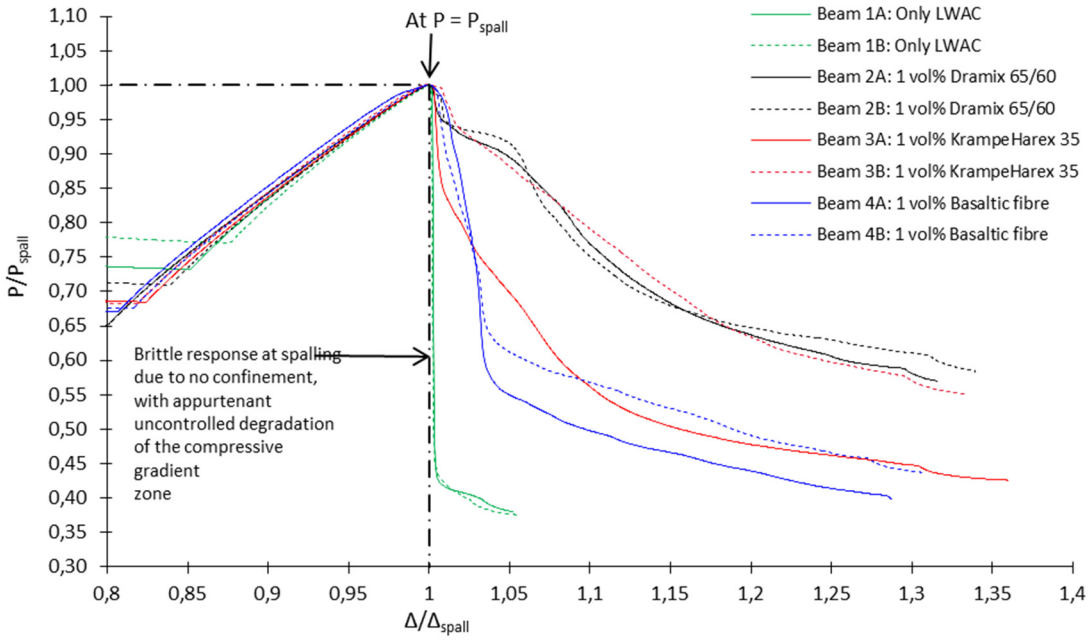

b) *Section of the normalized load-time curves around* P_{spall}

Figure 3.2*: Load-time curves for all beams*

3.3 Concrete and steel strains

3.3.1 Strain curves

Experimental moment-strain and time-strain relation for one reference beam with only LWAC, beam 1A, and for one beam with steel fibre of length 60mm, beam 4A, are shown in Figure 3.3 and 3.4 respectively. Analogous to the load-displacement relationships shown in Chapter 3.2, the figures show the improvement of the flexural response after spalling of the compression zone by introducing the fibres.

Figure 3.4 shows how fibre and stirrups, i.e. cross-section with confined fibre reinforced LWAC in the compression gradient zone, result in a more ductile behaviour after spalling. However, after reaching the spalling moment, M_{spall}, the bending capacity is reduced with corresponding large strains in the compressive zone. The positive values show the compressive strains in the LWAC (IT3-IT4), while the tensile strains at the bottom of the beams (IT1-IT2) are shown in negative values.

Strain curves for all beams are given in Appendix A2.

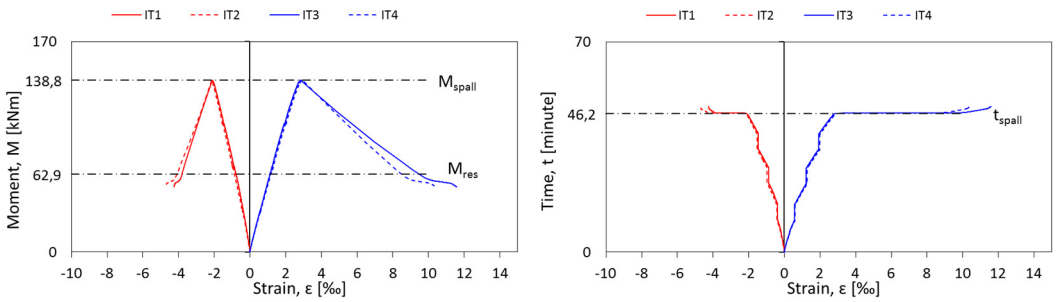

a) *Moment-strain curves* ***b)*** *Time-strain curves*

Figure 3.3*: Strain curves for Beam 1A, only LWAC.*

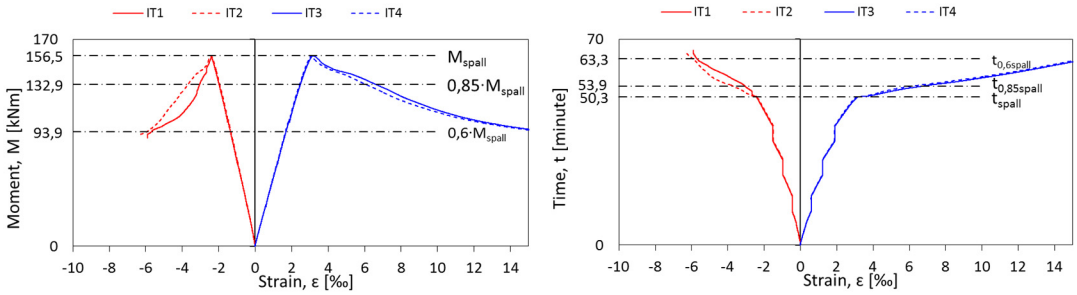

a) *Moment-strain curves* ***b)*** *Time-strain curves*

Figure 3.4*: Strain curves for Beam 2A, 1 vol% Dramix 65/60*

3.3.2 Strain distribution in cross-section at peak-loads

The strain distributions in cross-section at spalling (P_{spall}) and after a load reduction corresponding to a moment capacity of 85% of the spalling capacity ($0{,}85M_{spall}$) are illustrated in front elevation for each beam in Figure 3.5 – 3.8. The calculated strain distribution at spalling, $P_{spall,calc}$, are also shown in the figures, and correspond quite well with the experiments, in the same way as the calculated capacity itself, i.e. the concrete compressive strain at spalling (from IT1 – IT4) correspond with the ultimate compressive strain, ε_{lcu3} (EC2), used in calculations, see Table 3.1.

From Figure 3.5 – 3.8 it appears that the response from the tensile reinforcement is elastic all the way up to P_{spall} for all beams, i.e. the beams can be characterized as over-reinforced. The collapse of the compression gradient zones of the beams after spalling is evident with a rotation centre localized close to the centre of the longitudinal tensile reinforcement.

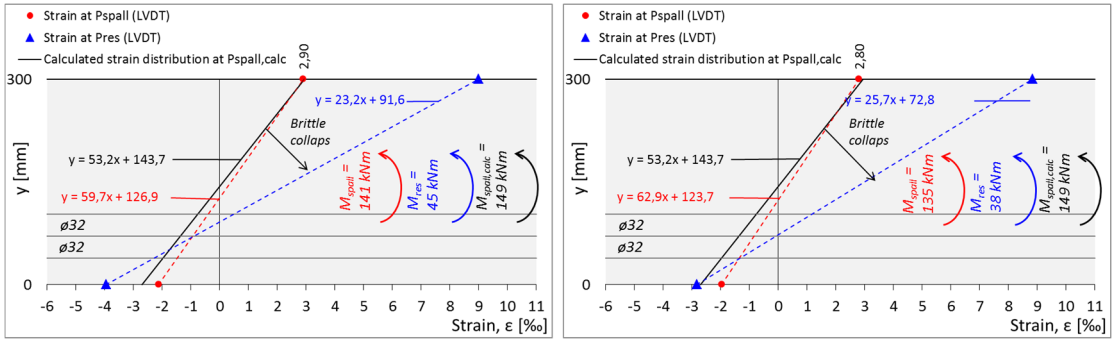

a) *Beam 1A* ***b)*** *Beam 1B*

Figure 3.5*: Beam 1A/1B – Only LWAC. Longitudinal strain distribution. Brittle collapse of the compression gradient zone from M_{spall} to M_{res}*

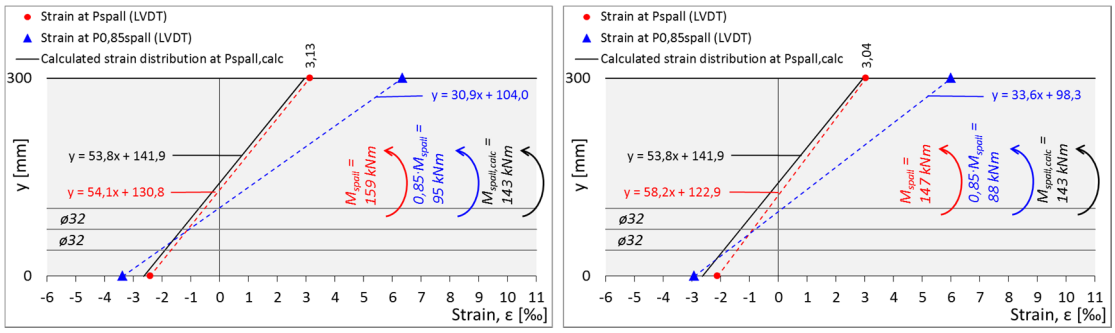

a) *Beam 2A* ***b)*** *Beam 2B*

Figure 3.6*: Beam 2A/2B – 1 vol% Dramix 65/60. Longitudinal strain distribution*

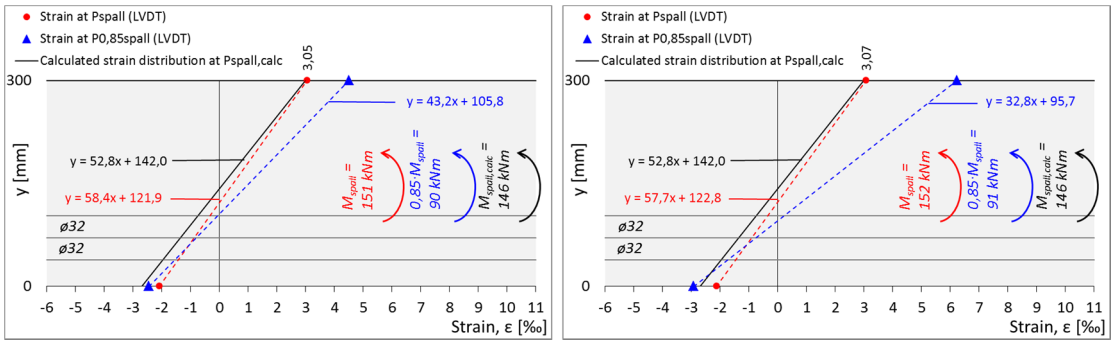

a) *Beam 3A* ***b)*** *Beam 3B*

Figure 3.7*: Beam 3A/3B – 1 vol% KrampeHarex/35. Longitudinal strain distribution*

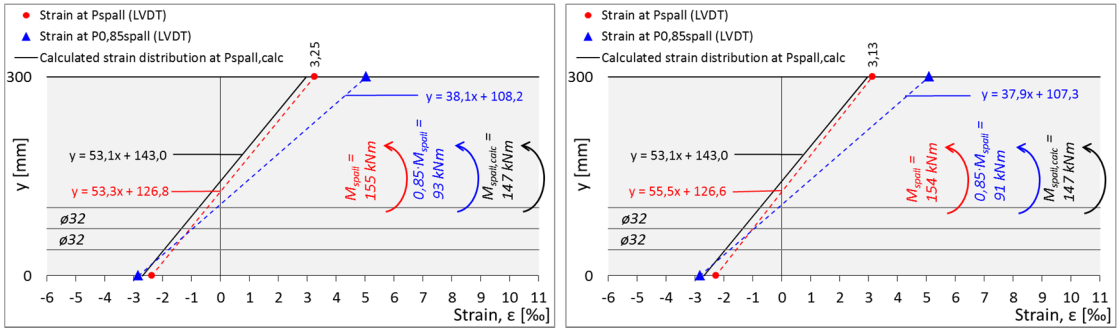

a) *Beam 4A* ***b)*** *Beam 4B*

Figure 3.8*: Beam 4A/4B – 1 vol% Basaltic fibre. Longitudinal strain distribution*

3.4 Failure mode and ultimate strength

The governing failure mode for all beams was typical bending failures for over-reinforced beams. The failure and spalling of the concrete cover are initiated and identified when horizontal cracks occurs in the compression zone. Depending on the degree of confinement, pictures in Figure 3.9 – 3.12 shows the typical differense in the the failure zone between the reference beam with only LWAC and beam with fibres. The picture of the beam with only LWAC is taken at the end of testing, while the pictures for the beams with fibre the pictures are at peak (spalling) load and approximately when the load is reduced to $0{,}85P_{spall}$. The spalling is much more severe in the beam without fibre than beams with fibres, where the cross-section remains much more intact. The failure zone without fibres is much more local and concentrated than with fibres where the zone is wider. From the figures it is clear that the size of the spalling zone in the longitudinal direction is typically limited by the distance of 800 mm between the fibreboards in the pure bending zone. Thus, these plates work as external confinement with respect to spalling. From the pictures it can be seen that in beams without fibres, the concrete cover is almost separated from the beams at peak loads. For beams with fibres there are only minor horizontal cracking in the compressive zone at peak load.

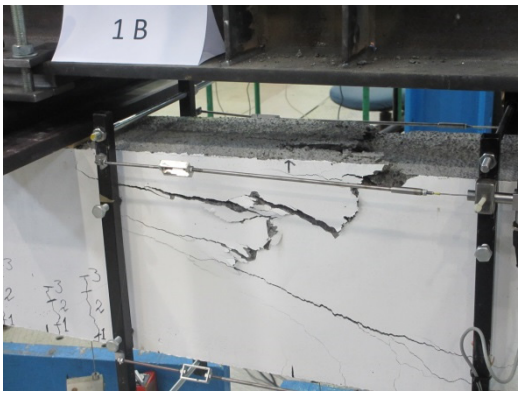

At the end of testing

***Figure 3.9**: Beam 1B. Only LWAC. Failure zone in beam*

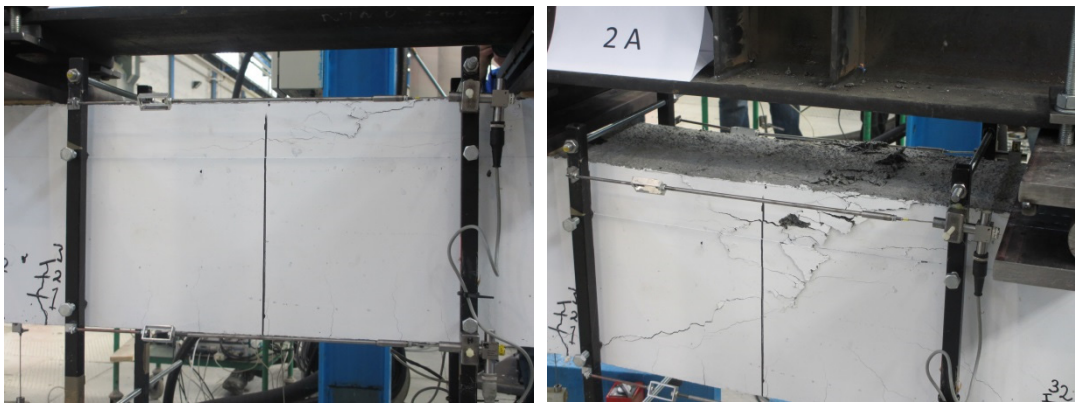

***a)** At P_{spall} = 103,0 kN, Δ_{peak} =25,1 mm* ***b)** At P~0,85· P_{spall} = 87 kN*

***Figure 3.10**: Beam 2B. Dramix 65/60 steel fibre. Failure zone in beam*

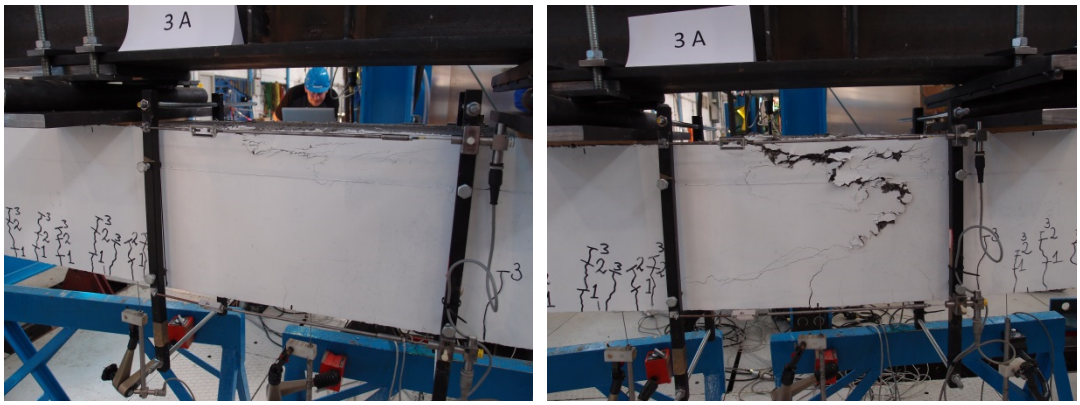

a) *At P_{spall} = 106,5 kN, Δ_{spall} =22,5 mm* ***b)*** *At P~0,85 · P_{spall} = 90 kN,*

Figure 3.11*: Beam 3A. CrampeHarex35. Failure zone in beam*

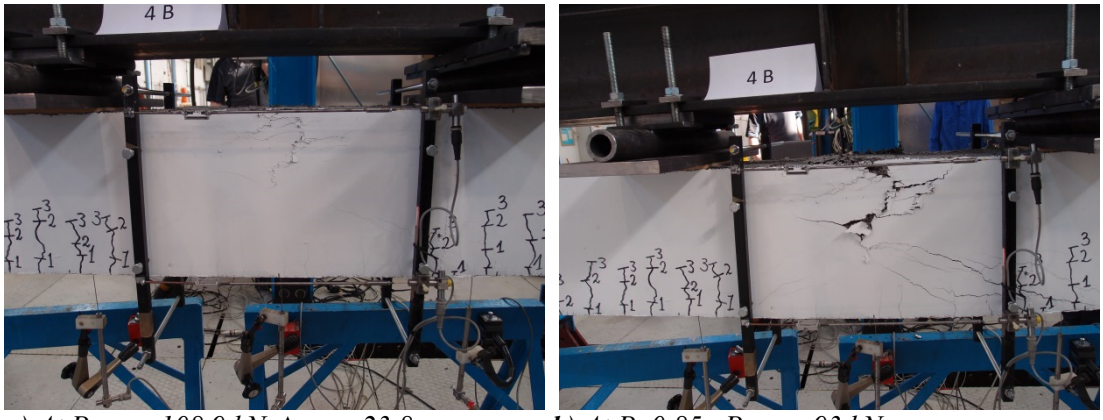

a) *At P_{spall} = 108,9 kN, Δ_{spall} =23,8 mm* ***b)*** *At P~0,85 · P_{spall} = 93 kN*

Figure 3.12*: Beam 4B. Baslatic fibre. Failure zone in beam*

To be able to compare the test results with theoretical prediction for bending capacity, the recommendations in EC2 were employed. The theoretical value for spalling and peak loads were calculated using the measured stress-strain relation for the reinforcement, see Figure 2.6, and the measured compressive strength, f_{lcm}, for LWAC, see Table 2.2. The compressive strain, at peak stress, ε_{lcu3}, were calculated according to EC2 based on the oven dry density, ρ, of the LWAC. The calculated strain in the tensile reinforcement was 1.5 ‰ at failure.

The calculation model for expected capacity, $P_{spall,calc}$, at the initiation of spalling (horizontal cracks), consider the equivalent rectangular stress diagram for concrete in compression according to EC2. The same model is used for all beams. Thus, the effect of confinement in the compressive zone is not taken into account. In Table 3.1 the theoretical predictions of the load capacity, $P_{spall,calc}$, are given and compared with the test results, P_{spall}. In general the agreement is good. Except for beams without fibre, the calculations slightly underestimate the capacity. Figure 3.20 shows the influence of compressive strength on the ratio of test to calculated capacities at spalling.

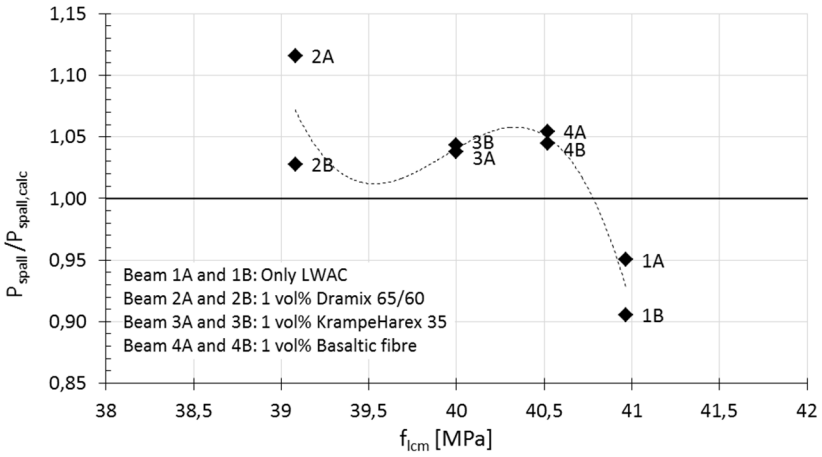

Figure 3.20: *Influence of compressive strength and fibre on the ratio of test to calculated capacities at spalling.*

4 Ductility

4.1 Ductility characteristics

Ductility is the ability for a structural member to deform inelastic without significant loss of strength. It can be measured at various levels in a structure - material, section, element or global. The most common way of quantifying ductility is to employ a ductility index, which on a sectional level often is defined as the ratio of curvature at crushing of concrete to that of yielding of reinforcement. In seismic design in Eurocode 8 where formation of yield hinges is important, the local sectional ductility index is defined with a post-peak value of 85 % of the maximum value in bending [31]. In this study the beams are over-reinforced meaning yielding of reinforcement cannot be used to find a ductility index. Instead a displacement ductility index, μ_i, is calculated as the ratio of the vertical mid span displacement in the post-peak response at 85% and 60% of the peak load to the displacement at peak load. The beams with only LWAC do not have any ductility at all due to the brittle failures.

Figure 4.1 presents the displacement ductility ratios for the beams with fibre. As expected they are not very large due to the drop in the capacity of the beams after reaching the peak load. Thus, the conclusion of this experimental investigation could be that fibres do not significantly improve the ductility in over-reinforced LWAC beams. Even the 60 mm long steel fibres could not be consider ductile in a structural design. However, the effect of fibres is also related to the curvature in the cross-section. With a higher curvature the ductility will also increase.

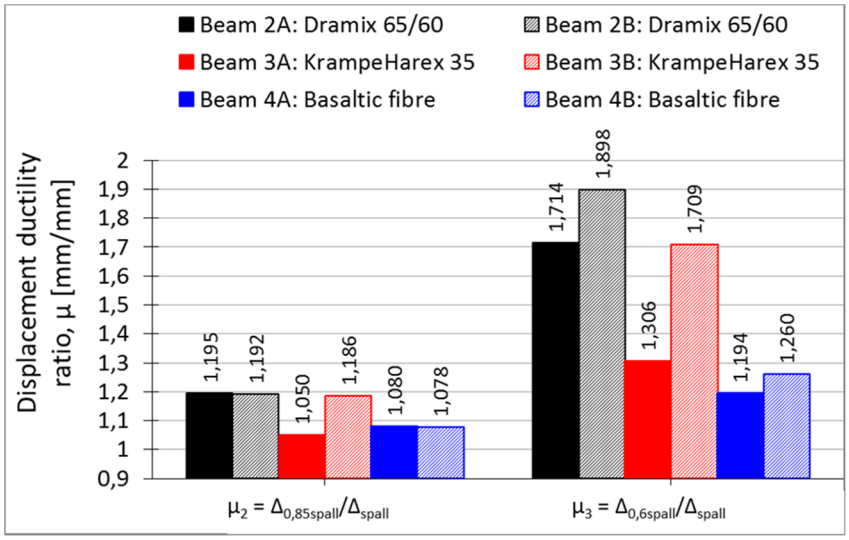

***Figure 4.1**: Displacement ductility ratio for all beams with fibres.*

4.2 Displacement relationships within the plastic hinge region

The rotational capacity of so called plastic hinge areas plays an important role in the analyses of ultimate load capacity and ductility of continuous beams and frames. By comparing the displacement relationships at mid span and at load-points for the over-reinforced beams with the same reinforcement ratio in this study, the different moment redistribution potential can be illustrated. For the beams in this study the reinforcement ratio are very high, and the plastic rotation capacity will depend almost completely on the limited plastic strain of the LWAC alone. Thus the different displacement relationships at peak loads are only related to the different confinement configurations in the compressive gradient zones.

Figure 4.2 shows a schematic diagram of how the relationships between displacements at mid span and at load-points is theoretically limited by a lower limit of 1,066 and an upper limit of 1,286. The lower limit assumes linear elastic material properties and constant bending stiffness in the beam. However, lower values appear before spalling due to non-linear stress-strain relationships in the compressive zone between the load points, which gives local and a distributed reduced stiffness in the bending zone. The upper limit represents a theoretical model with a local concentrated plastic hinge with a much lower bending stiffness than the rest of the beam.

Figure 4.3 – 4.11 present test results of the ratio of mid span to load-point displacement, $\Delta_{IT6}/\Delta_{IT5,IT7}$, with respect both to mid span displacement, Δ_{IT6}, and time, t, during testing. The load response is also given in the figures. At load levels below spalling the ratio is typical in the range 1,06 – 1,07, which is close to expected values. After spalling the ratio increases. For beams with only LWAC, beam 1A and 1B, there is a pronounced increase just after spalling before levelling out with a ratio of approximately 1,18. Such a shape of the graph is in accordance with formation of a very local plastic hinge.

From Figure 4.3 it can clearly be seen that the beams with fibres have a much more gradual increase in the ratio after spalling load. Hence, the beams are able to activate a larger area during formation of the plastic zone in the middle part of the beam. Since the loading (displacement) rate was the same for all beams during testing, the relationship between displacement ratio and testing time gives valuable information.

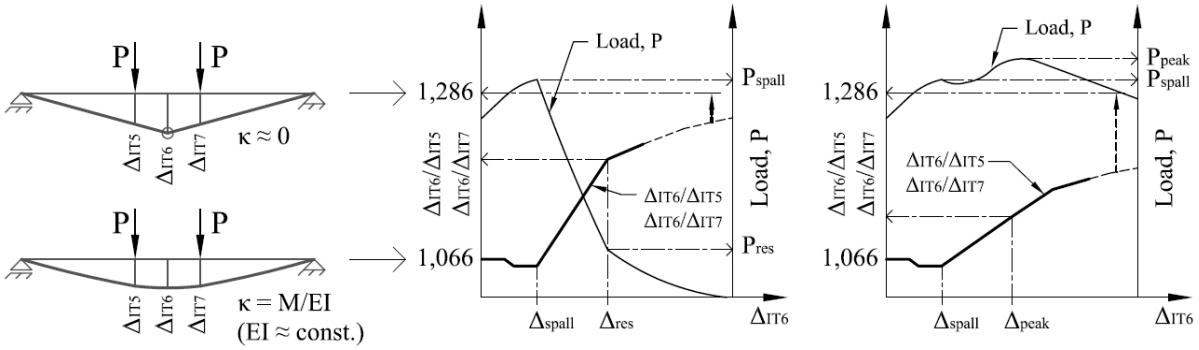

a) *Principle drawing* ***b)*** *Response beam 1* ***c)*** *Response beam 2-4*

Figure 4.2*: Schematic relationships between displacement at mid span and at load-point*

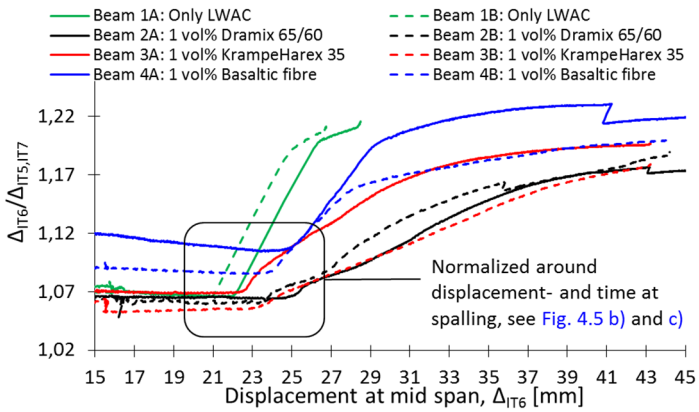

a) *Relationship all beam*

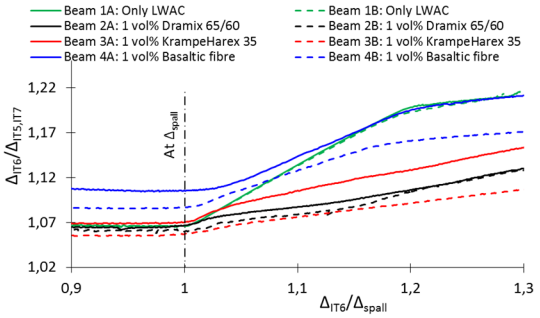

b) *Normalized around* Δ_{spall}

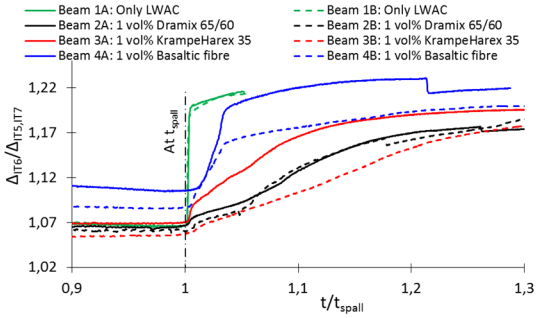

c) *Normalized around* t_{spall}

Figure 4.3*: All beams. Relationship between displacement at mid span and at load points*

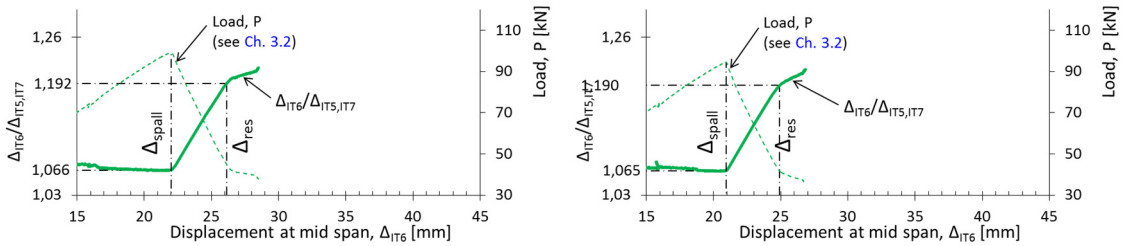

a) *Beam 1A* ***b)*** *Beam 1B*

Figure 4.4*: Beam 1 – Only LWAC. Ratio between displacement at mid span and at load-points, including appurtenant load response*

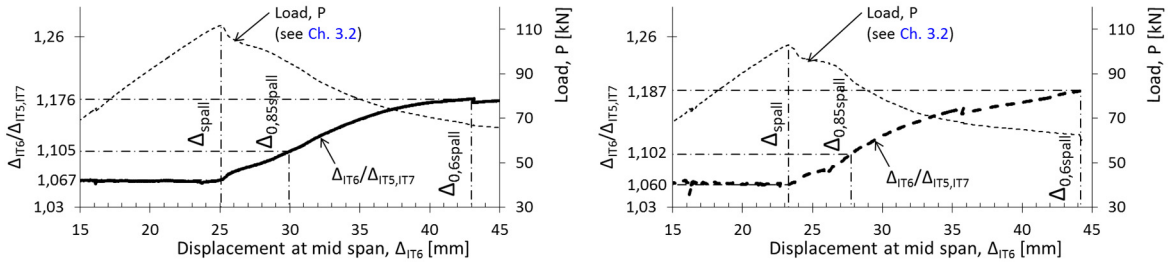

a) *Beam 2A* ***b)*** *Beam 2B*

Figure 4.5*: Beam 2 – Dramix 65/60. Ratio between displacement at mid span and at load-points, including appurtenant load response*

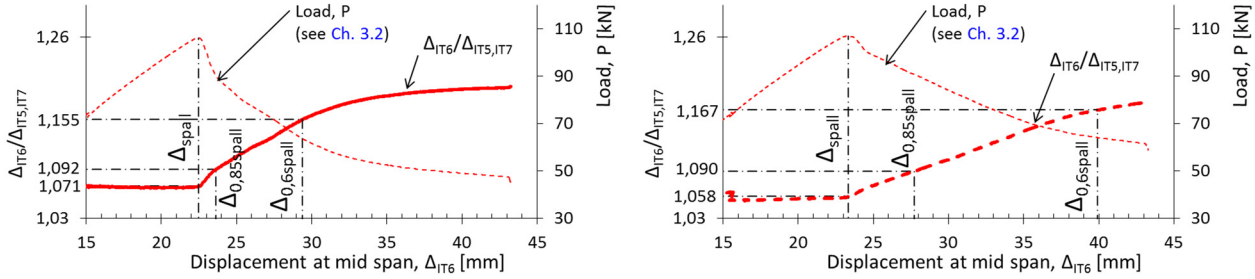

a) *Beam 3A* ***b)*** *Beam 3B*

Figure 4.6*: Beam 3 – KrampeHarex 35. Ratio between displacement at mid span and at load- points, including appurtenant load response*

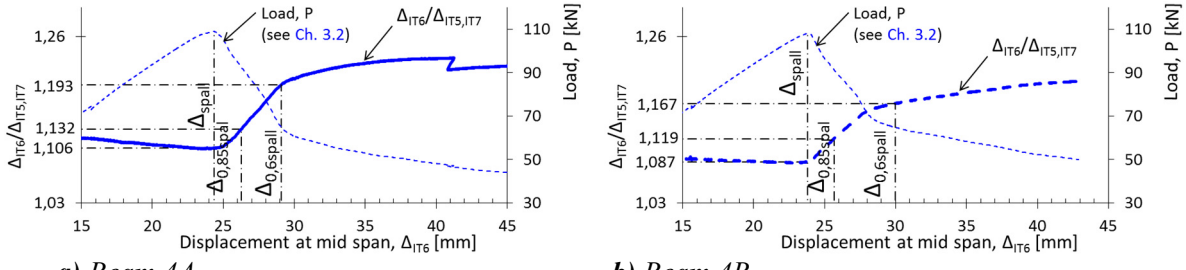

a) *Beam 4A* ***b)*** *Beam 4B*

Figure 4.7*: Beam 4 – Basaltic fibre. Ratio between displacement at mid span and at load-points, including appurtenant load response*

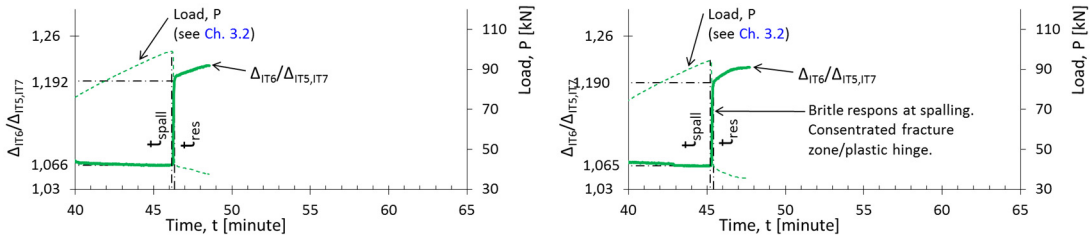

a) *Beam 1A* ***b)*** *Beam 1B*

Figure 4.8*: Beam 1 – Only LWAC. Ratio between displacement at mid span and at load-points, including appurtenant load response*

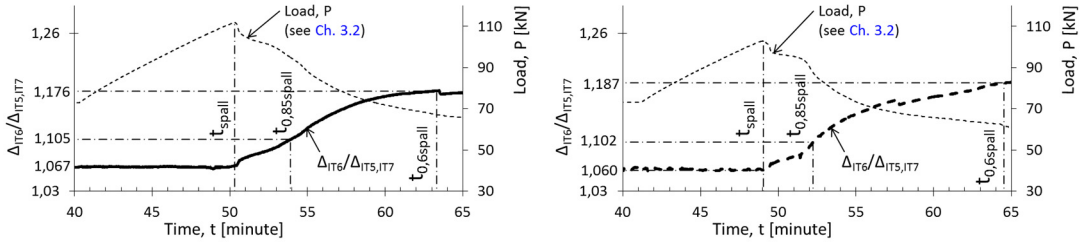

a) *Beam 2A* ***b)*** *Beam 2B*

Figure 4.9*: Beam 2 – Dramix 65/60. Ratio between displacement at mid span and at load-points, including appurtenant load response*

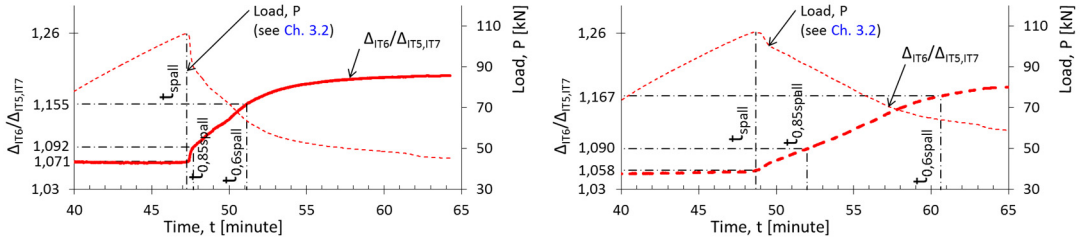

a) *Beam 3A* ***b)*** *Beam 3B*

Figure 4.10*: Beam 3 – KrampeHarex 35. Ratio between displacement at mid span and at load-points, including appurtenant load response*

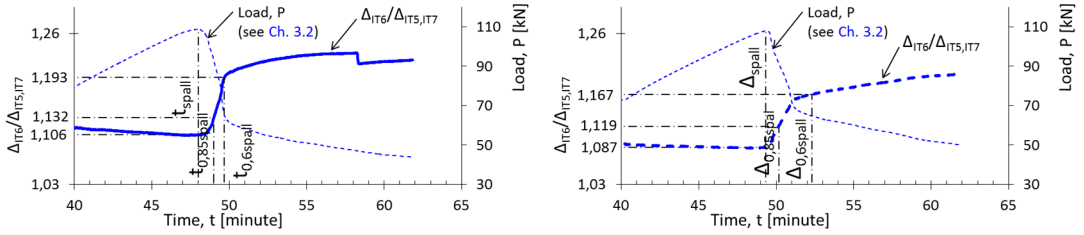

a) *Beam 4A* ***b)*** *Beam 4B*

Figure 4.11*: Beam 4 – Basaltic fibre. Ratio between displacement at mid span and at load-points, including appurtenant load response*

5 Conclusion

In this study eight over-reinforced lightweight aggregate concrete beams were subjected to four-point bending. The main goal was to study the confinement effects of different type of fibres zone. The effect was not as large as anticipated before the study. Other studies have shown considerably effect on the ductility be employing fibres. However, among parameters influencing the ductility are the size of cross-section, curvature and amount of fibre. So other configurations of the beams in this project could achieve better ductility

In theory over-reinforced lightweight aggregate concrete structures are not ductile. The experiment shows how it is possible to obtain some ductile response of such structures by increasing the compressive ductility properties with different types of fibre.

The fibres increase the load capacity of the beams by approximately 10%, indicating the fibres do contribute to a confinement effect. As expected, the two reference beams (beam 1A and 1B) with only LWAC in the compression zone, had a brittle post-peak response, i.e. no post-peak deformability and a very steep descending branch immediately after initiation of spalling of the concrete cover. However, also the beams with fibre show a drop in the capacity after peak load even if they introduce a softer transition after spalling of the concrete cover. Even if the beams with fibre are not completely brittle they cannot be considered ductile in a structural design.

6 Acknowledgements

The authors would like to acknowledge the financial support from COIN, the Concrete Innovation Centre, which is a centre for research based innovation with funding from the Norwegian Research Council and industrial partners, and the assistance of Stian Hoff, Torgeir Steen, Johann Helgi Oskarsson and Angel Arcadi Sorni Moreno for carrying out the experimental work as part of their master thesis.

References

[1] ACI Committee 213. Guide for Structural Lightweight Aggregate Concrete (ACI 213R-03). American Concrete Institute. Farmington Hills, MI, United States: American Concrete Institute; 2003.
[2] Attard MM, Setunge S. Stress-strain relationship of confined and unconfined concrete. ACI Materials Journal. 1996;93:432-42.
[3] Cheong HK, Zeng H. Stress-strain relationship for concrete confined by lateral steel reinforcement. ACI Materials Journal. 2002;99:250-5.
[4] Mander JB, Priestley MJN, Park R. Observed stress-strain behavior of confined concrete. J Struct Eng. 1988;114:1827-49.
[5] Sheikh SA, Toklucu MT. Reinforced concrete columns confined by circular spirals and hoops. ACI Struct J. 1993;90:542-53.
[6] Mander J, Priestley M, Park R. Theoretical Stress-Strain Model for Confined Concrete. J Struct Eng. 1988;114:1804-26.
[7] Schumacher P. Rotation Capacity of Self-compacting Steel Fiber Reinforced Concrete: Technical University of Delft; 2006.
[8] Balaguru P, Foden A. Properties of fiber reinforced structural lightweight concrete. ACI Struct J. 1996;93:62-78.
[9] Balendran RV, Zhou FP, Nadeem A, Leung AYT. Influence of steel fibres on strength and ductility of normal and lightweight high strength concrete. Building and Environment. 2002;37:1361-7.
[10] Campione G, La Mendola L. Behavior in compression of lightweight fiber reinforced concrete confined with transverse steel reinforcement. Cement and Concrete Composites. 2004;26:645-56.
[11] Standards Norway. NS-EN 1992-1-1:2004+NA:2008. Eurocode 2: Design of concrete structures - General rules and rules for buildings. Norway: Standards Norway; 2008.
[12] Kim Y-J, Harmon TG. Analytical model for confined lightweight aggregate concrete. ACI Struct J. 2006;103:263-70.
[13] Kosaka Y, Tanigawa Y, Hatanaka S. Lateral confining stresses due to steel fibres in concrete under compression. International Journal of Cement Composites and Lightweight Concrete. 1985;7:81-92.
[14] Mangat PS, Motamedi Azari M. Influence of steel fibre and stirrup reinforcement on the properties of concrete in compression members. International Journal of Cement Composites and Lightweight Concrete. 1985;7:183-92.
[15] Sin LH, Huan WT, Islam MR, Mansur MA. Reinforced lightweight concrete beams in flexure. ACI Struct J. 2011;108:3-12.
[16] Ahmad SH, Barker R. Flexural behavior of reinforced high-strength lightweight concrete beams. ACI Struct J. 1991;88:69-77.
[17] Ahmad SH, Batts J. Flexural behavior of doubly reinforced high-strength lightweight concrete beams with web reinforcement. ACI Struct J. 1991;88:351-8.
[18] Altun F, Aktaş B. Investigation of reinforced concrete beams behavior of steel fiber added lightweight concrete. Construction and Building Materials. 2013;38:575-81.
[19] Carmo RNF, Costa H, Simões T, Lourenço C, Andrade D. Influence of both concrete strength and transverse confinement on bending behavior of reinforced LWAC beams. Engineering Structures. 2013;48:329-41.
[20] Øverli JA, Jensen TM. Increasing ductility in heavily reinforced LWAC structures. Engineering Structures. 2014;62–63:11-22.
[21] Oskarsson JH. The effect of fibres on the comrpessive ductility og Lightweight aggregate concrete. Department of Structural Engineering: Norwegian University of Science and Technology; 2013.

[22] Hoff S, Steen T. Ductility of lightweight aggregate concrete. Department of Structural Engineering: Norwegian University of Science and Technology; 2013.
[23] Moreno AAS. Improved in ductility of lightweight aggregate concrete. Department of Structural Engineering: Norwegian University of Science and Technology; 2013.
[24] Standards Norway. NS-EN 12390-3:2009. Testing hardened concrete - Part 3: Compressive strength of test specimens Norway: Standards Norway; 2009.
[25] Standards Norway. NS-EN 12390-9:2009. Testing hardened concrete - Part 7: Density of hardened concrete. Lysaker: Standards Norway; 2009.
[26] Standards Norway. NS-EN ISO 15630-1. Steel for the reinforcement and prestressing of concrete - Test methods - Part 1: Reinforcing bars, wire rod and wire. Norway: Standards Norway; 2010.
[27] Standards Norway. NS-EN 14651:2005+A1:2007. Test method for metallic fibre concrete - Measuring the flexural tensile strength (limit of proportionality (LOP), residual). Lysaker: Standards Norway; 2008.
[28] Kanstad T. Proposal for norwegian guidelines for design, execution and control of fibre reinforced concrete. SINTEF Building and Infrastructure; 2011.
[29] fédération internationale de béton. Model Code 2010 : Final draft. Lausanne, Switzerland: fib; 2012. p. 2 b.
[30] Standard Norge. NS-EN 1992-1-1:2004+NA:2008. Eurocode 2: Design of concrete structures - General rules and rules for buildings. Norway: Standard Norge; 2008.
[31] Standards Norway. NS-EN 1998-1:2004+NA:2008. Eurocode 8: Design of structures for earthquake resistance. Part 1: General rules, seismic actions and rules for buildings. Norway: Standards Norway; 2008.

Appendices

Appendix A1: Load curves

Remark: Mid span displacement from inductive transducer no. IT6, see Figure 2.5.

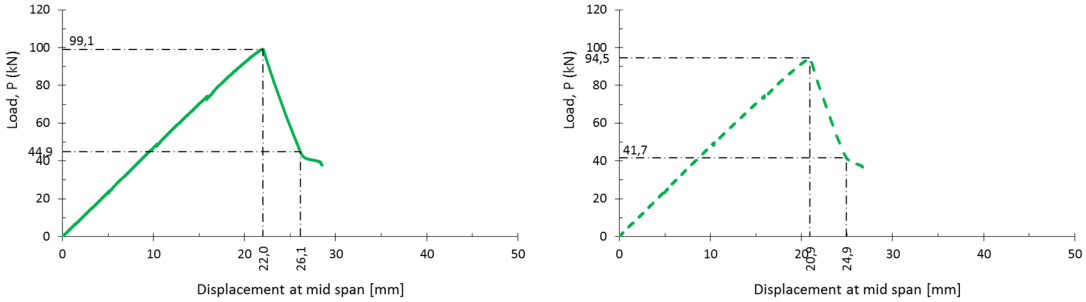

a) *Beam 1A* ***b)*** *Beam 1B*

Figure A1.1*: Beam 1A/1B – Only LWAC. Load-displacement curves*

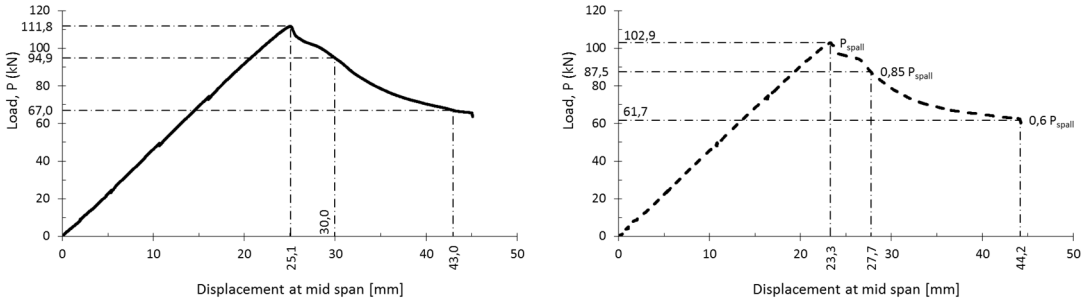

a) *Beam 2A* ***b)*** *Beam 2B*

Figure A1.2*: Beam 2A/2B – 1 vol% Dramix 65/60. Load-displacement curves*

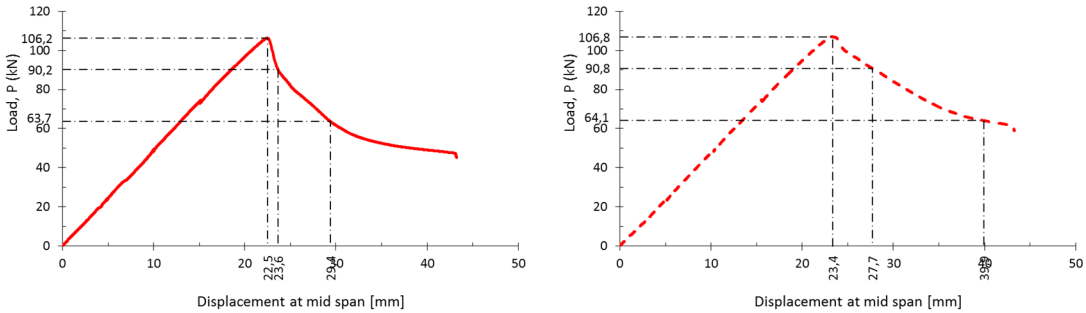

a) *Beam 3A* ***b)*** *Beam 3B*

Figure A1.3*: Beam 3A/3B – 1 vol% Dramix 65/35. Load-displacement curves*

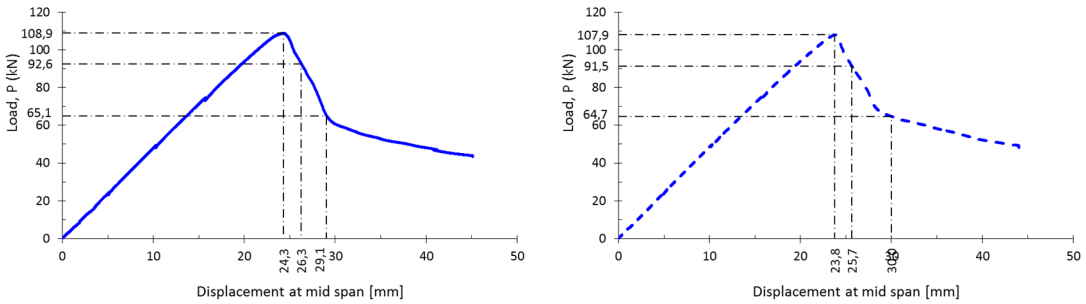

a) *Beam 4A* ***b)*** *Beam 4B*

Figure A1.4*: Beam 4A/4B – 1 vol% Basaltic fibre. Load-displacement curves*

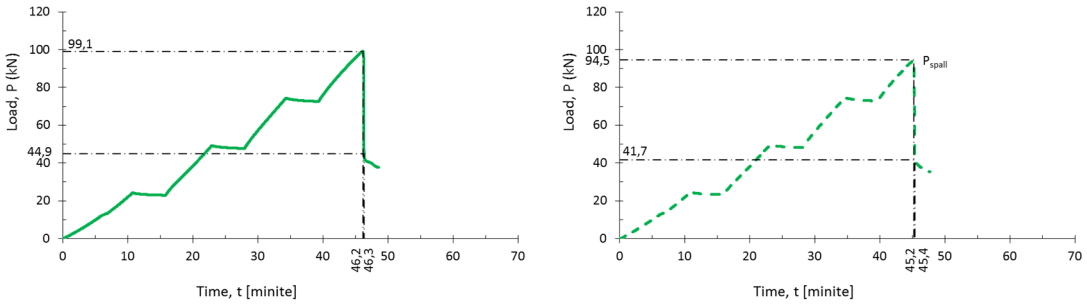

a) *Beam 1A* ***b)*** *Beam 1B*

Figure A1.5*: Beam 1A/1B – Only LWAC. Load-time curves*

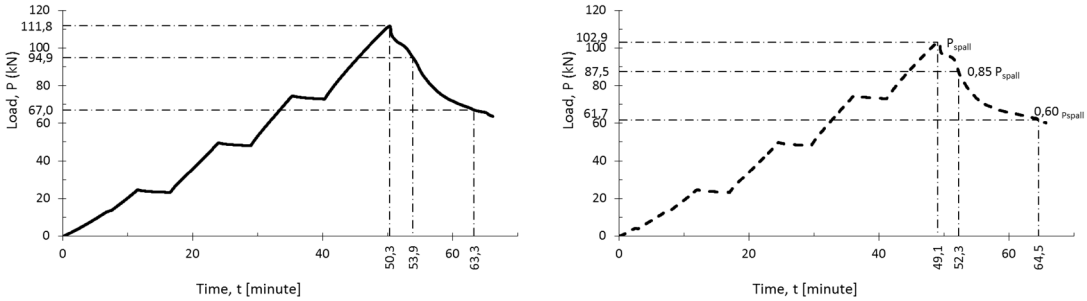

a) *Beam 2A* ***b)*** *Beam 2B*

Figure A1.6*: Beam 2A/2B – 1 vol% Dramix 65/60. Load-time curves*

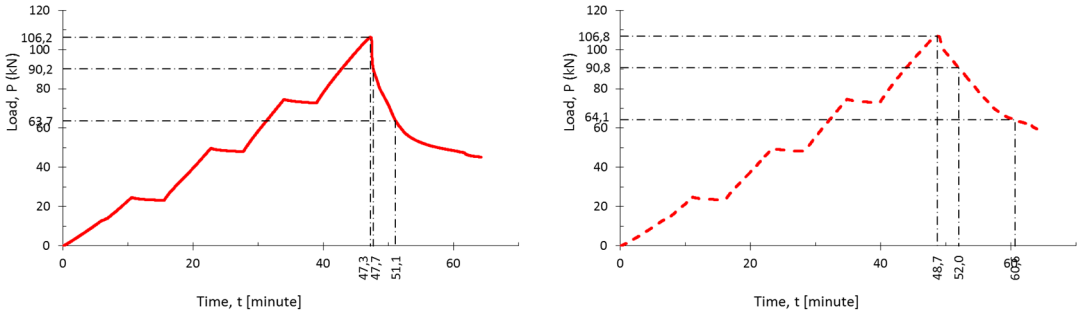

a) *Beam 3A* ***b)*** *Beam 3B*

Figure A1.7*: Beam 3A/3B – 1 vol% Dramix 65/35. Load-time curves*

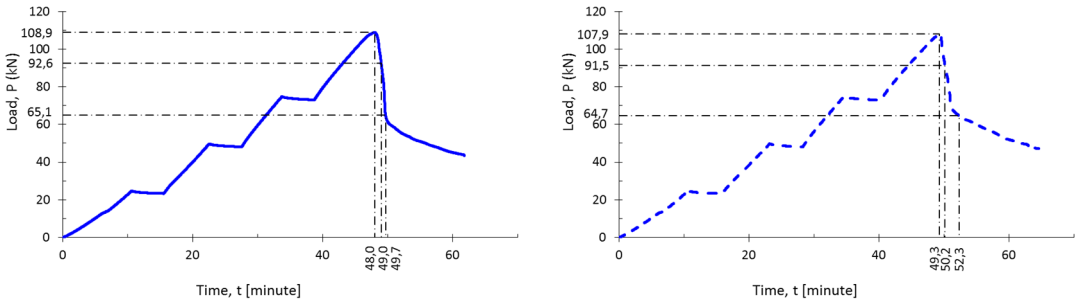

a) *Beam 4A* ***b)*** *Beam 4B*

Figure A1.8*: Beam 4A/4B – 1 vol% Basaltic fibre. Load-time curves*

Appendix A2: Strain curves

Remark: Location of inductive transducers IT1-IT4 (LVDT), see Figure 2.8 and 2.9.

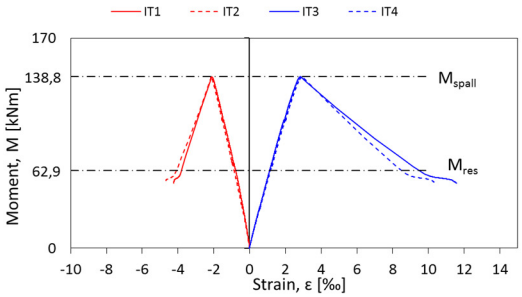

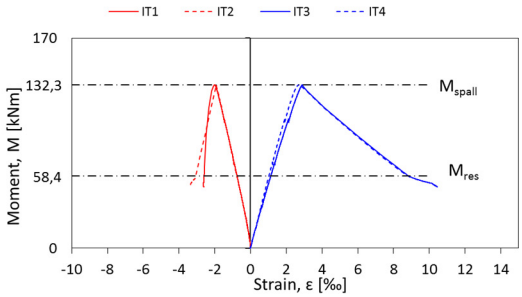

a) *Beam 1A (same as Figure 3.4 a)* ***b)*** *Beam 1B*

Figure A2.1*: Beam 1A/1B – Only LWAC. Moment-strain curves*

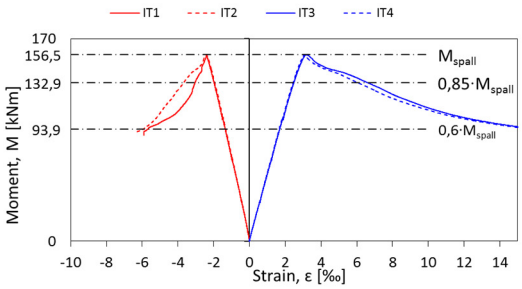

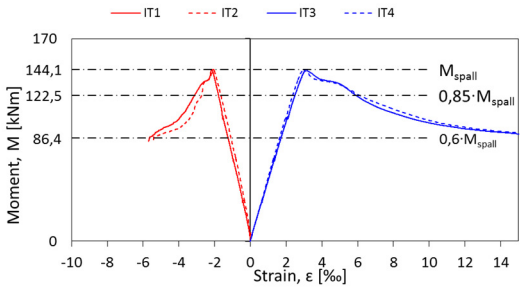

a) *Beam 2A (same as Figure 3.5 a)* ***b)*** *Beam 2B*

Figure A2.2*: Beam 2A/2B – 1 vol% Dramix 65/60. Moment-strain curves*

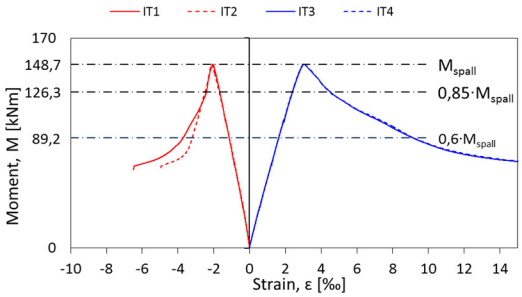

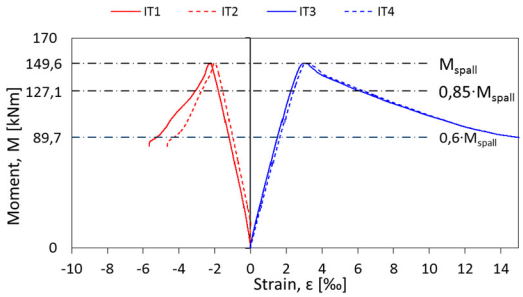

a) *Beam 3A* ***b)*** *Beam 3B*

Figure A2.3*: Beam 3A/3B – 1 vol% Dramix 65/35. Moment-strain curves*

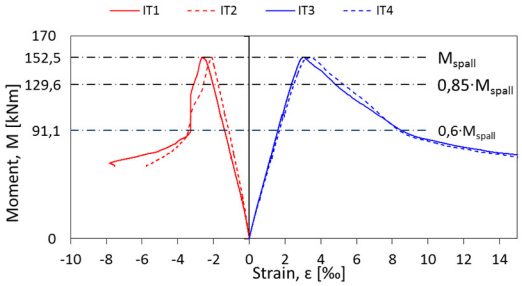

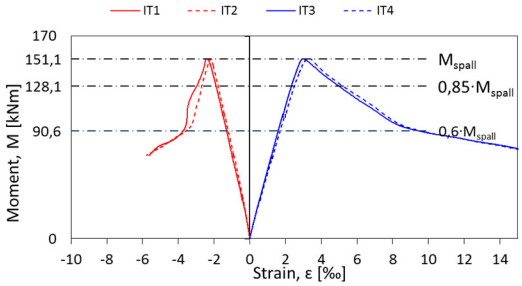

a) *Beam 4A* ***b)*** *Beam 4B*

Figure A2.4*: Beam 4A/4B – 1 vol% Basaltic fibre. Moment-strain curves*

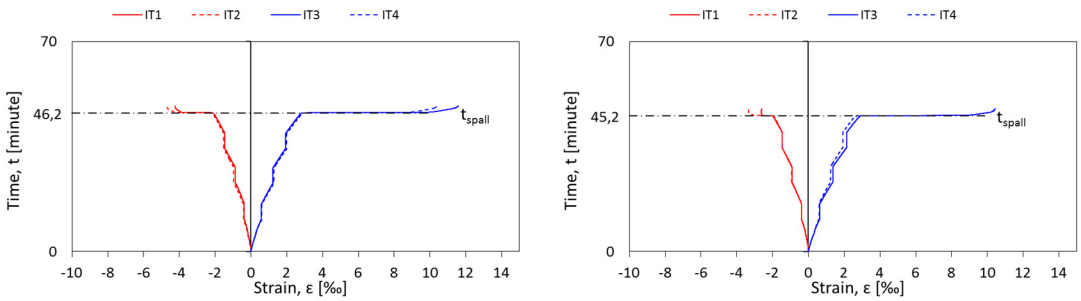

a) *Beam 1A (same as Figure 3.4 b)* ***b)*** *Beam 1B*

Figure A2.5*: Beam 1A/1B – Only LWAC: Time-strain curves*

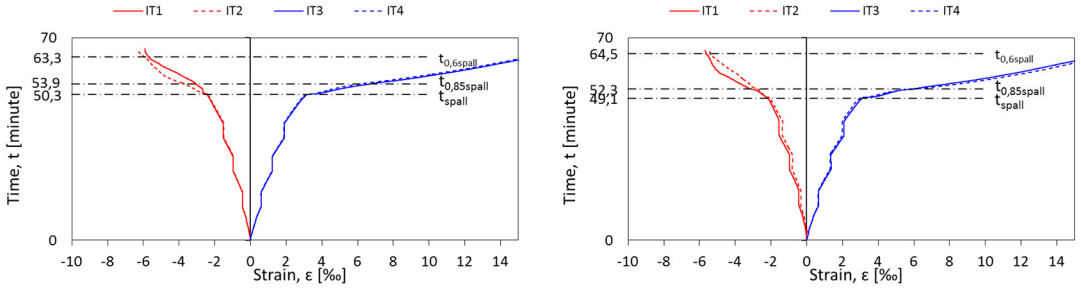

a) *Beam 2A (same as Figure 3.5 b)* ***b)*** *Beam 2B*

Figure A2.6*: Beam 2A/2B – Fibre: Time-strain curves*

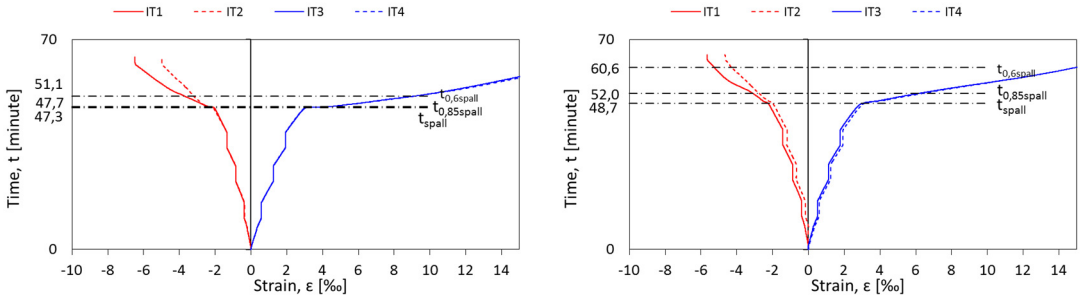

a) *Beam 3A* ***b)*** *Beam 3B*

Figure A2.7*: Beam 3A/3B – Stirrups: Time-strain curves.*

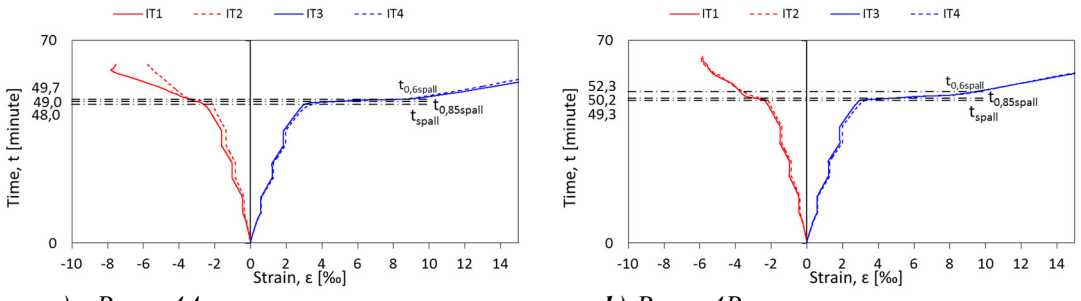

a) *Beam 4A* ***b)*** *Beam 4B*

Figure A2.8*: Beam 4A/4B – Fibre + stirrups. Time-strain curves*

Appendix A3: Number of fibres in small scale beams

***Table A3-1**: Number of fibres in small scale beams*

Small scale beam no.		Number of fibres							
		X1	X2	X3	X4	X5	X6	Mean value	Std. (%)
Beam 2B	Upper (25mm)	76	70	80	52	64	100	74	22,0
	Middle (100mm)	34	105	88	75	50	54	68	39,1
	Lower (25mm)	72	60	80	102	121	105	90	25,6
	Total	182	235	248	229	235	259	231	11,5
Beam 4B	Upper (25mm)	100	150	126	193	194	197	160	25,7
	Middle (100mm)	55	184	160	182	183	217	164	34,4
	Lower (25mm)	104	190	190	186	184	200	176	20,2
	Total	259	524	476	561	561	614	499	25,3
Beam 4	Upper (25mm)	74	49	45	41	50	69	55	24,7
	Middle (100mm)	86	56	51	50	65	84	65	24,7
	Lower (25mm)	96	36	36	60	42	62	55	41,6
	Total	256	141	132	151	157	215	175	28,0

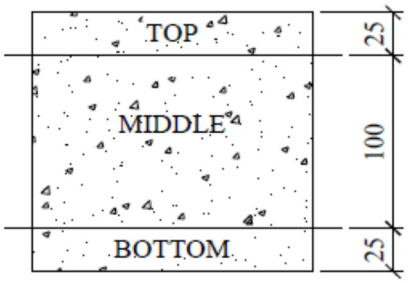

***Figure A3-1**: Specimen for fibre counting*

SINTEF Building and Infrastructure is the third largest building research institute in Europe. Our objective is to promote environmentally friendly, cost-effective products and solutions within the built environment. SINTEF Building and Infrastructure is Norway's leading provider of research-based knowledge to the construction sector. Through our activity in research and development, we have established a unique platform for disseminating knowledge throughout a large part of the construction industry.

COIN – Concrete Innovation Center is a Center for Research based Innovation (CRI) initiated by the Research Council of Norway. The vision of COIN is creation of more attractive concrete buildings and constructions. The primary goal is to fulfill this vision by bringing the development a major leap forward by long-term research in close alliances with the industry regarding advanced materials, efficient construction techniques and new design concepts combined with more environmentally friendly material production.